



## Quantitative proteomic analysis of MDCK cell adhesion†

Cite this: *Mol. Omics*, 2021, 17, 121

Xuanqing Ye,<sup>a</sup> Jiamin Wang,<sup>ab</sup> Zilin Qiao,<sup>ab</sup> Di Yang,<sup>b</sup> Jiao Wang,<sup>c</sup> Ayimuguli Abudureyimu,<sup>d</sup> Kun Yang,<sup>d</sup> Yuping Feng,<sup>d</sup> Zhongren Ma<sup>ab</sup> and Zhenbin Liu<sup>ib</sup> \*<sup>ab</sup>

MDCK cells are a key reagent in modern vaccine production. As MDCK cells are normally adherent, creation of suspension cells for vaccine production using genetic engineering approaches is highly desirable. However, little is known regarding the mechanisms and effectors underlying MDCK cell adhesion. In this study, we performed a comparative analysis of whole protein levels between MDCK adhesion and suspension cells using an iTRAQ-based (isobaric tags for relative and absolute quantitation) proteomics approach. We found that expression of several proteins involved in cell adhesion exhibit reduced expression in suspension cells, including at the mRNA level. Proteins whose expression was reduced in suspension cells include cadherin 1 (CDH1), catenin beta-1 (CTNNB1), and catenin alpha-1 (CTNNA1), which are involved in intercellular adhesion; junction plakoglobin (JUP), desmoplakin (DSP), and desmoglein 3 (DSG3), which are desmosome components; and transglutaminase 2 (TGM2) and alpha-actinin-1 (ACTN1), which regulate the adhesion between cells and the extracellular matrix. A functional verification experiment showed that inhibition of E-cadherin significantly reduced intercellular adhesion of MDCK cells. E-Cadherin did not significantly affect the proliferation of MDCK cells and the replication of influenza virus. These findings reveal possible mechanisms underlying adhesion of MDCK cells and will guide the creation of MDCK suspension cells by genetic engineering.

Received 14th May 2020,  
Accepted 10th November 2020

DOI: 10.1039/d0mo00055h

rsc.li/molomics

## Introduction

Influenza-related illnesses cause an estimated 100 000 hospitalizations and tens of thousands of deaths in the United States annually. In response to rapid antigenic drift of influenza viruses, the most effective prevention approach has been the distribution of trivalent inactivated viral vaccines, which are traditionally produced in embryonated chicken eggs.<sup>1</sup> However, in the event of a pandemic outbreak, this egg-based production system may not be adequate to meet increased demand. Among the potential alternatives for vaccine production, use of characterized, immortalized cell lines (particularly MDCK, VERO,

and PER.C6) has been investigated.<sup>2</sup> These cell lines have been found to produce consistently high viral titers.<sup>3,4</sup>

The MDCK cell line was developed by Madin and Darby in 1958 from kidney tissue from a Cocker Spaniel. MDCK cells are epithelioid cells and usually exhibit adhesive growth when cultured *in vitro*. Due to their high viral production efficiency, rapid proliferation, and low mutation rate, MDCK cells are considered an efficient host for influenza virus production<sup>5,6</sup> MDCK cells are widely used for the amplification and purification of multiple viruses, such as avian influenza virus (AIV), reovirus, adenovirus, canine parvovirus (CPV), and feline pan leukopenia virus (FPLV).<sup>7,8</sup> The majority of traditional MDCK cell culture methods utilize a two-dimensional single cell layer grown adherently in culture medium containing serum.<sup>6</sup> In adherent culture of a single cell layer, cell proliferation is limited by substrate surface area and thus is difficult to implement in large-scale production. Trypsin digestion of the cell can also increase the complexity and time of vaccine production.<sup>9</sup> Suspension culture avoids the restriction of the cell growth surface, allowing for mass production of cells and vaccines. At present, MDCK suspension cells are primarily obtained by serum-free domestication culture,<sup>10,11</sup> but the conventional domestication process used to create suspension cells is lengthy and expensive. Cell activity also decreases with repeated

<sup>a</sup> Gansu Tech Innovation Center of Animal Cell, Biomedical Research Center, Northwest Minzu University, Lanzhou 730030, China.  
E-mail: liuzhenbin6@163.com

<sup>b</sup> Key Laboratory of Biotechnology and Bioengineering of State Ethnic Affairs Commission, Biomedical Research Center, Northwest Minzu University, Lanzhou 730030, China

<sup>c</sup> Laboratory of Molecular Neural Biology, School of Life Sciences, Shanghai University, Shanghai, 200444, China

<sup>d</sup> Life Science and Engineering College, Northwest Minzu University, Lanzhou 730030, China

† Electronic supplementary information (ESI) available. See DOI: 10.1039/d0mo00055h

passage of cells. Establishment of suspension cell lines that grow in serum-free media and generate high cell-specific yields would be of enormous economic importance.

Therefore, modifying adherence-related genes in MDCK cells by genetic engineering in order to establish a stable MDCK suspension cell line has significant potential to aid industrialization of vaccine production.<sup>5,8,9</sup> However, this approach requires knowledge of the proteins that are required for adhesive function in MDCK cells and an understanding of how these proteins affect cell adhesion. Cell–cell adhesion is essential for the organization and maintenance of complex tissues in multicellular organisms. Cell–cell and cell–extracellular matrix adhesion depends on cell-specific adhesive proteins as well as cytoplasmic proteins that regulate signaling and actin cytoskeletal dynamics.<sup>12</sup> Given that both cell–cell and cell–substrate adhesion must be dynamic (to allow tissue growth and remodeling) and stable (to provide mechanical strength), these interactions are highly regulated.<sup>13,14</sup> A wide variety of cell adhesion mechanisms are involved in the assembly of cell–cell and cell–substrate adhesions. Different cell adhesion molecules (CAMs) along with cell skeleton structure determines the adhesion properties of the cell and the structure of the tissue. Many proteins have been found to be involved in cell adhesion, including integrins, selectin, immunoglobulins, and cadherins. Different tissues and cells may express different adhesion proteins, and adhesion proteins display tissue specificity.<sup>15–18</sup> Identification and characterization of proteins that significantly affect the adhesion properties of MDCK cells is essential for modification of their cell attachment properties. It has been reported that transfer of the gene encoding human sialic acid transferase (sial7e) into MDCK cells can reduce MDCK cell adhesion.<sup>19</sup> However, there are few reports of adherent proteins of MDCK cells, and little is known about the adhesion mechanisms of MDCK cell lines. There have several reports that describe successful generation of MDCK suspension cells by domestication and continuous passage in culture.<sup>11,20</sup> In previous studies, our research team obtained a MDCK cell line, deemed MDCK<sub>SUS</sub>, with stable suspended growth in serum-free media by manual domestication screening. Undomesticated adherent cells were labeled as MDCK<sub>ADH</sub>. MDCK cell line adaptation was carried out using a two-step strategy: first, adaptation to growth in low serum suspension medium and then growth in suspension.<sup>10</sup> Tissue-like cell aggregates formed a growth-supporting microenvironment during the adaptation process.

In this study, we used comparative proteomic analysis of MDCK<sub>ADH</sub> cells and MDCK<sub>SUS</sub> cells using isobaric tags for relative and absolute quantitation (iTRAQ) technology. A total of 643 proteins with significantly different expression levels were detected. Compared with MDCK<sub>ADH</sub> cells, 389 proteins were up-regulated and 254 were down-regulated in MDCK<sub>SUS</sub> cells. Using protein function, localization, and changes in protein expression, we prioritized 12 proteins associated with cell adhesion. The reduction in expression of these proteins in suspension cells was further validated at the transcriptional level by real-time quantitative PCR (RT-qPCR). The expression

of these proteins in adherent cells was significantly greater than that in suspension cells, further supporting their role in adhesion and as candidate targets for genetic engineering of MDCK suspension cells.

## Methods

### Cell lines and culturing

MDCK adhesion cells (MDCK<sub>ADH</sub>) (CCL-34, ATCC) were cultivated in DMEM medium (Lanzhou Bailing Biotechnology Co., Ltd, BGL M101.01) with 10% fetal bovine serum (CellMax, SA311.01) in T-square flasks (Corning, 430641) at 5% CO<sub>2</sub> and 37 °C. The MDCK suspension cell line (MDCK<sub>SUS</sub>) was acquired by domestication in previous work by our laboratory.<sup>10,20–23</sup> The MDCK<sub>SUS</sub> cells were cultivated in serum-free SFM-MDCK medium (CellMax, CFM414.08) in shake flasks (Corning, #431401) at 5% CO<sub>2</sub>, 37 °C, and 120 rpm. Experiments were performed using three biological replicates with independent cultures. Experiments were performing using MDCK<sub>ADH</sub> cells and MDCK<sub>SUS</sub> cells.

### Protein extraction and quantification

For each sample, 100 µL was combined with 50 µL of SDT (4% [w/v] SDS, 0.1 M Tris HCl pH 7.6, 0.1 M DTT) lysate. After sonication, the cells were boiled for 10 min and centrifuged at 16 000 × *g* at 4 °C. Protein was quantified using the BCA method.

### Protein digestion and peptide desalting

For each sample, 300 µg was used for enzymatic hydrolysis. DTT was added to 100 mM, and the sample was boiled for 5 min and cooled to room temperature. Then, 200 µL of UA buffer (8 M urea, 150 mM Tris–HCl, pH 8.0) was added and the sample was mixed, transferred to a 10 kD ultrafiltration centrifuge tube, and centrifuged at 12 000 × *g* for 15 min. UA buffer (15 µL) was added and the sample was centrifuged for 15 min, and the filtrate discarded. Next, 100 µL of 50 mM IAA (in UA) was added, and the sample was shaken at 600 rpm for 1 min, incubated at room temperature for 30 min while protected from light, and centrifuged at 12 000*g* for 10 min. The sample was washed twice with 100 µL UA buffer and centrifuged at 12 000 × *g* for 10 min each. The sample was then washed twice with NH<sub>4</sub>HCO<sub>3</sub> buffer (100 µL) and centrifuged at 14 000 × *g* for 10 min. Trypsin buffer (6 µg trypsin in 40 µL NH<sub>4</sub>HCO<sub>3</sub> buffer) was added, and the sample was shaken at 600 rpm for 1 min and then incubated at 37 °C for 16–18 h. The collection tube was exchanged, and the sample was centrifuged at 12 000 × *g* for 10 min. Then, TFA solution was added to the filtrate to a final concentration of 0.1%, and the sample was desalinated using a C18 cartridge. Samples were quantified by measuring the OD280.

### iTRAQ peptide labeling and peptide fractionation

For each sample, 100 µg of peptides were labeled using the 8-plex iTRAQ reagent according to the manufacturer's instructions

(AB Sciex, Framingham, MA, USA). Each group of labeled peptides was mixed in equal amounts, and the dried peptides were fractionated using a High-pH reversed-phase column (Pierce™ High pH Reversed-Phase Peptide Fractionation Kit, ThermoFisher). Three sample from the MDCKADH group were labeled with mass 113, 114, and 115 isobaric iTRAQ tags, while the other three samples from the MDCKsus group were labeled with mass 116, 117, and 118 isobaric iTRAQ tags. The six iTRAQ reagent-labeled samples were then pooled into a single vial. The collected samples were combined into 15 fractions, and the peptides of each fraction were dried and reconstituted in 0.1% FA for LC-MS analysis.

### LC-MS/MS analysis

The peptide-segment solution was analyzed by LC-MS/MS. The samples were labeled in triplicate, and were analyzed by mass spectrometry a total of 15 times. The HPLC liquid phase system Easy nLC was used for separation. Solution A contained 0.1% formic acid, and solution B contained 0.1% formic acid-85% acetonitrile. Samples were loaded onto a trap column (2 cm × 100 μm, 5 μm-C18) and a Thermo Scientific EASY column (75 μm, 120 mm, 3 μm-C18) for separation, with a flow rate of 300 nl min<sup>-1</sup>. The linear gradient of the solution was as follows: 0–2 min, 5% to 8% solution B; 2–42 min, 8% to 23% solution B; 42–50 min, 23% to 40% solution B; 50–52 min, 40 to 100% solution B; and 52–60 min, hold at 100% solution B. The chromatographic column was balanced with 95% solution A. The peptide fraction was separated by chromatography and analyzed on a Q-Exactive Plus mass spectrometer (Thermo Scientific) by tandem mass spectrometry. The analysis time was 60 min, the detection method was positive ion, and the mother ion scan range was 300–1800 *m/z*. The mass-charge ratio (*m/z*) of peptides to fragments was collected according to the following method: 20 fragment images were collected after each full scan (MS2 scan HCD). The first-order mass spectrum resolution was 70 000 at an *m/z* of 200. The AGC target was 1E6, and the maximum IT was 50. The second-order mass spectrum resolution was 17 500 at an *m/z* of 200. The AGC target was 1e5, and the maximum IT was 50. The MS2 activation type was HCD, the isolation window was 1.6 thin, and the normalized collision energy was.<sup>24,35</sup> In this study, variable modifications were defined as oxidation of methionine and iTRAQ 8-plex labeled tyrosine, while lysine and the N-termini of peptides labeled by iTRAQ 8-plex and carbamidomethylation on cysteine were specified as fixed modifications. For peptide and protein identification, the false discovery rate (FDR) was set to 1%.

### Database searching

The resulting LC-MS/MS raw file was imported into MaxQuant software (version 1.6.0.16) for database retrieval. The database used by uniprot-canis+lupus-29580-20180207. A FASTA-formatted list of *Canis lupus familiaris* proteins can be retrieved from Uniprot at <https://www.uniprot.org/uniprot/?query=taxonomy:9615>.<sup>24</sup>

### Real-time quantitative PCR analysis

We prioritized twelve adhesion-related genes in MDCK cells identified by iTRAQ proteomic analysis and verified their mRNA expression by qPCR. Total RNA was isolated from adherent and suspended cells using TRIzol in three independent experiments. The concentration and quality of each total RNA sample was measured using a BioPhotometer (Eppendorf). The  $A_{260}/A_{280}$  values for all samples were 1.8–2.0, and nucleic acid electrophoresis was used to further verify the purity. One μg of total RNA from each sample was used to synthesize cDNA using the iScript™ cDNA Synthesis Kit (Bio-Rad) according to the manufacturer's instructions. The cDNA was stored at –20 °C until further use. SYBR Green RT-qPCR assays were performed using the Bio-Rad iCycler iQ5 Real-Time PCR System. The primers were shown in Table S1 (ESI†). The transcript encoding β-actin was also amplified as an internal reference. DEPC water was used as a no-template negative control. The relative copy number of each gene was calculated according to the 2<sup>-ΔΔCT</sup> comparative CT method. Statistically significant differences were examined by paired *t*-test in GraphPad Prism 5.0 software. *p* values < 0.05 were considered statistically significant.<sup>25</sup>

### Western blot analysis

The cells were washed with ice-cold PBS gently, added 100 μl per well cell lysis buffer (Beyotime, Co., Ltd Shanghai, China) 30 min. Sample of cytosolic protein was formed by centrifugation at 12 000*g* for 10 min and protein concentration were determined by BCA method. The proteins were separated by 8% SDS-PAGE and then transferred to a PVDF membranes (Millipore, Bedford, MA). Western blot analysis was performed using the following primary antibodies and dilutions: anti-TGM2 (1:200 dilution, Thermo Fisher), E-cadherin antibodies (1:20000 dilution, BD) and β-Actin primary antibodies (1:1000 dilution, Cell Signaling) at 4 °C for overnight. After washing, the membranes were incubated with anti-mouse HRP-conjugated secondary antibody (1:10 000 dilution, Jackson) for 1 hour at room temperature. Results were visualized by using ELC detecting kit (PerkinElmer, Inc., MA) and Tanon 5500 gel imaging system (Tanon Science & Technology Co., Ltd Shanghai, China).

### Knockdown of CDH1

MDCK<sub>ADH</sub> cells were seeded in a 12-well plate (2 × 10<sup>5</sup> per well) and cultured in DMEM medium containing 10% FBS and 1% penicillin–streptomycin solution for 24 h. Cells were infected with lentivirus containing CDH1 shRNAs or a control vector at an MOI of 100. Lentivirus was removed 24 h after infection, and culture medium was added. After culture for another 24 h, cells were screened with 7 μg ml<sup>-1</sup> puromycin. After five consecutive cell passages, mRNA and protein levels of CDH1 were detected to verify creation of knockdown cells for functional verification experiments. CDH1 knockdown cells were designated as shCDH1 and the vector control cells as shCon.

### Cell adhesion assay

Untransfected MDCK<sub>ADH</sub> cells (Blank), shCon cells, and shCDH1 cells were seeded in a 96-well plate that was already covered with a layer of MDCK cells at  $1 \times 10^4$  cells per well.<sup>11</sup> Cells were incubated at 37 °C in a 5% CO<sub>2</sub> incubator for 1 h and then washed twice with PBS. The transferred expression vector carries a GFP tag, and fluorescence microscopy was used to observe the number of adherent cells. A cell counting kit (CCK8, Meliubio, China) was used to measure the number of adherent cells and calculate the adhesion rate.<sup>26</sup> The cell adhesion rate was calculated as:

$$\text{Cell adhesion rate} = \frac{(\text{experimental group OD}_{450} - \text{blank group OD}_{450})}{(\text{control group OD}_{450} - \text{blank group OD}_{450})} \times 100\%$$

### IAV infection and titer assay

shCon and shCDH1 MDCK cells in logarithmic phase were seeded at  $2 \times 10^5$  cells per well in 12-well plates and incubated at 37 °C in 5% CO<sub>2</sub> until the cell density reached 90%. Medium was removed and cells were washed twice with PBS. Cells were infected with Influenza A/Puerto Rico/8/34 (A/PR/8/34) H1N1 virus in serum-free medium containing TPCK-trypsin ( $2 \mu\text{g ml}^{-1}$ ) at an MOI of 0.001 and were incubated at 37 °C in a 5% CO<sub>2</sub> incubator for 1 h. After 48 h of infection, virus was collected for titer determination.

Virus titer was determined using a Tissue Culture Infective Dose (TCID<sub>50</sub>) assay. Briefly, MDCK cells were seeded in 96-well plates at a density of 25 000 cells per well. The next day, the cells were washed twice with serum-free medium. A series of ten-fold dilutions of stocks of allantoic fluid or cell culture supernatant ranging from  $10^{-1}$  to  $10^{-8}$  was prepared in serum-free medium with  $2 \mu\text{g ml}^{-1}$  L-1-tosylamide-2-phenylethyl chloromethyl ketone-treated trypsin (TPCK-trypsin). The cells were infected with each diluted virus stock in triplicate. After 48 h of culture,

the cells were analyzed for the virus' cytopathic effect (CPE), and TCID<sub>50</sub> was calculated using the Reed–Muench method.<sup>27</sup>

## Results

### Overview of iTRAQ data analysis

MaxQuant software was used to analyze iTRAQ-labeled proteomics data. The iTRAQ analysis of the proteomes of MDCK<sub>ADH</sub> and MDCK<sub>SUS</sub> cells identified 3543 distinct proteins, including 2973 proteins that were quantified. Proteins that displayed a greater than 1.2-fold change in expression (up- or down-regulation) and a *p*-value less than 0.05 were considered to be significantly differentially expressed.<sup>28,29</sup> Fold changes in expression between the two cell types and *p*-values calculated using *t* tests were plotted on volcano plots. Compared with MDCK<sub>ADH</sub> cells, we find that MDCK<sub>SUS</sub> cells significantly differentially express 643 proteins. Among these, 389 proteins were up-regulated and 254 were down-regulated (Fig. 1). In clustering analysis of differential protein expression data, data are visualized in two dimensions, protein sample and quantity of protein. Clustering of the target proteins allows us to distinguish different expression patterns in the proteome. Proteins with similar expression patterns may have a similar function or be involved in the same biological pathway. In our data, we observe high similarity in expression patterns within three biological repeats and low similarity between MDCK<sub>ADH</sub> and MDCK<sub>SUS</sub>. Thus, the changes in protein expression we identified are likely reflective of the biological treatment of the samples.

### Gene ontology enrichment analysis

Gene ontology is a classification system that provides a dynamic standardized vocabulary to describe gene function. Gene ontology uses three types of designations to describe the

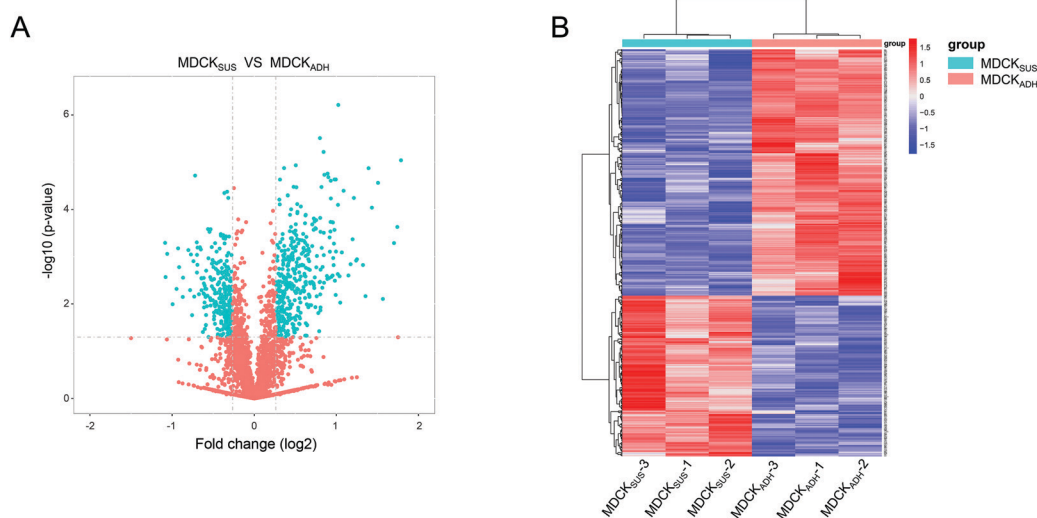


**Fig. 1** Overview of comparative proteomic analysis of MDCK<sub>ADH</sub> and MDCK<sub>SUS</sub> cell lines. (A) Volcano plot representing the significance and magnitude of the protein level changes in the MDCK<sub>SUS</sub> vs. MDCK<sub>ADH</sub> statistical comparison. The green point is the significantly different protein. (B) Heatmap of the significantly altered proteins between MDCK<sub>ADH</sub> and MDCK<sub>SUS</sub> cell. The color key indicates the relative abundance of proteins.

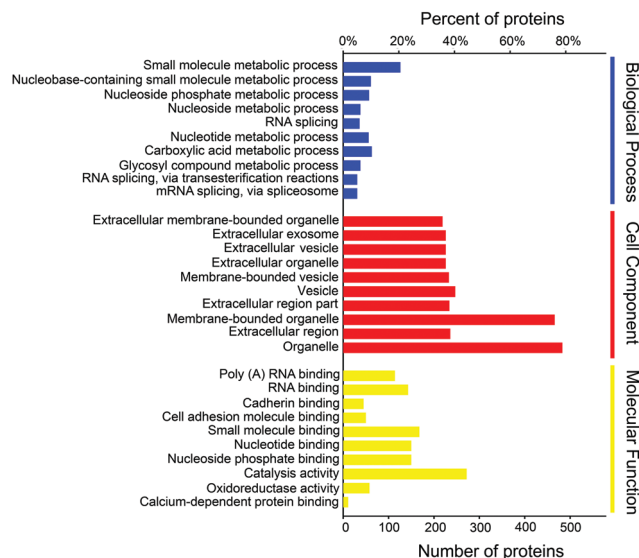


Fig. 2 Gene ontology (GO) analysis of significantly altered proteins between MDCK<sub>ADH</sub> and MDCK<sub>SUS</sub> cell. Classification of these proteins in different categories based on biological process, cellular component and molecular function.

biology of genes and gene products: biological processes, molecular function, and cellular components. Normally, significant enrichment of GO annotations is analyzed by Fisher's exact test. In our analysis, a total of 1250 GO terms were assigned to the 643 differentially expressed proteins. The top 10 GO terms in each group, as determined by the *P*-value of their difference between groups, are presented in Fig. 2. Within the biological processes group, many of the significant proteins identified are involved in cellular metabolism. Our results suggest that although the suspension cells were obtained by domestication, their metabolism was significantly affected in this process. In the cell component group, we observed significant differences in the expression levels of many proteins that localize to vesicles and exosomes. Exosome function is an area of interest in the field of cell biology.<sup>30</sup> Exosomes can

modulate inter- and intracellular signaling and participate in a variety of physiological and pathological processes.<sup>31</sup> Our analysis revealed that after inducing suspension in MDCK cells, the expression of many exosome proteins changed significantly. How these changes in protein expression affect exosome function in MDCK cells requires further study.

### Screening of adhesion-related proteins

We prioritized proteins likely to be major contributors to MDCK cell adhesion using multiple criteria. First, using the Biological Process gene ontology terms, we identified 50 proteins with significantly different expression between MDCK<sub>SUS</sub> cells and MDCK<sub>ADH</sub> cells that are associated with cell adhesion. Second, considering the direct interactions between cells and between cells and the extracellular matrix, most of the cell adhesion-related proteins localize to the cell membrane structure or bind to membrane proteins. Thus, we also selected proteins located on the cell membrane or related to the cell membrane. Third, we expect that expression of adhesion molecules or proteins that positively regulate adhesion function would be significantly reduced in suspension cells. Using the above criteria along with changes in protein expression, we narrowed our list of differentially expressed proteins to 12 proteins that met the above three screening conditions (Table 1). Among these, cadherin-1 (CDH1), desmoglein-3 (DSG3), and epithelial cell adhesion molecule (EPCAM) have been reported to function as typical CAMs in other cells. The remaining proteins have also been shown to be involved in cell adhesion. In particular, studies have shown that catenin  $\beta$  (CTNNB1),<sup>32</sup> catenin  $\alpha$  (CTNNA1),<sup>33</sup> junction plakoglobin (JUP),<sup>34</sup> and desmoplakin (DSP)<sup>33</sup> are not CAMs but still play important roles in cell adhesion.

### Validation of gene expression by RT-qPCR

We hypothesized that the observed changes in protein expression were likely due to changes at the mRNA level. We used RT-qPCR to analyze changes in mRNA levels that may underlie the changes in protein expression of our 12 proteins of interest.

Table 1 Twelve cell adhesion-related proteins were identified that their expression levels were significantly reduced in MDCK<sub>SUS</sub> cells

Gene ID <sup>a</sup>	Protein name	Score <sup>b</sup>	Coverage <sup>c</sup> (%)	Peptides <sup>d</sup>	Ratio <sup>e</sup> (MDCK <sub>SUS</sub> /MDCK <sub>ADH</sub> )				<i>p</i> -Values <sup>g</sup>
					iBR1 <sup>f</sup>	iBR2	iBR3	Means $\pm$ SD	
480522	Junction plakoglobin (JUP)	268.48	54.7	30	0.644	0.517	0.566	0.576 $\pm$ 0.052	0.0007
477032	Catenin $\beta$ -1 (CTNNB1)	118.68	30	20	0.766	0.749	0.751	0.755 $\pm$ 0.008	0.0004
474698	Catenin $\alpha$ -1 (CTNNA1)	296.22	48.7	34	0.792	0.780	0.795	0.789 $\pm$ 0.007	0.0016
479937	Calponin-3 (CNN3)	12.799	10.9	3	0.727	0.680	0.808	0.738 $\pm$ 0.053	0.0020
442858	Cadherin-1 (CDH1)	122.13	19.3	15	0.767	0.925	0.743	0.812 $\pm$ 0.081	0.0383
488207	Desmoplakin (DSP)	323.31	35.4	100	0.782	0.764	0.716	0.754 $\pm$ 0.028	0.0012
480369	Actinin alpha 1 (ACTN1)	323.31	52.5	39	0.858	0.767	0.837	0.821 $\pm$ 0.039	0.0029
478767	Dipeptidyl peptidase 4 (DDP4)	21.162	18.4	12	0.794	0.743	0.750	0.762 $\pm$ 0.023	0.0023
485867	Transglutaminase 2 (TGM2)	5.9027	3.8	3	0.481	0.571	0.392	0.481 $\pm$ 0.073	0.0027
403980	Caveolin-1 (CAV1)	35.553	51.1	9	0.902	0.707	0.758	0.788 $\pm$ 0.083	0.0151
481360	Epithelial cell adhesion molecule (EPCAM)	35.73	41.5	9	0.803	0.856	0.763	0.807 $\pm$ 0.038	0.0311
403470	Desmoglein-3 (DSG3)	162.82	17.6	12	0.878	0.787	0.796	0.82 $\pm$ 0.041	0.0033

<sup>a</sup> Gene ID according to NCBI database. <sup>b</sup> MaxQuant score (3.0 or more) from MaxQuant search engine (v.1.5.2.8) were considered successfully identified. <sup>c</sup> The percentage of the protein sequence covered by identified peptides. <sup>d</sup> Peptides, number of peptide spectrums matched for each protein. <sup>e</sup> Ratio, intensities of identified protein-MDCK<sub>SUS</sub> cells to MDCK<sub>ADH</sub> cells. <sup>f</sup> iBR, independent biological replicates 1, 2 and 3. <sup>g</sup> *p*-Values, the proteins that had a statistically significant (*p* < 0.05).

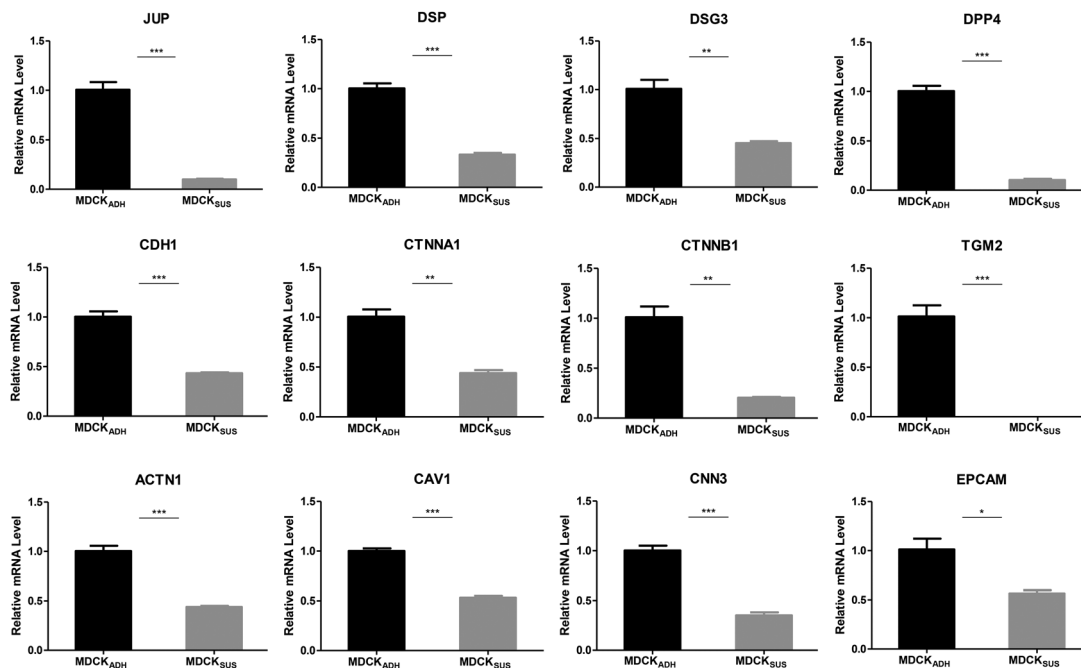


Fig. 3 The relative mRNA expression of screened adhesion-related proteins revealed by real-time quantitative PCR. Data are shown as mean  $\pm$  SD (standard deviation) of tissues from three separate individuals.

As shown in Fig. 3, the mRNA levels of all of the selected genes were significantly down-regulated in MDCK<sub>SUS</sub> cells, which was consistent with the protein expression trends observed by iTRAQ analysis.

### Protein interaction network analysis

To further describe possible relationships between the screened adhesion-related proteins, we constructed a protein–protein interaction network using the STRING database version 9.0 (Fig. 4).

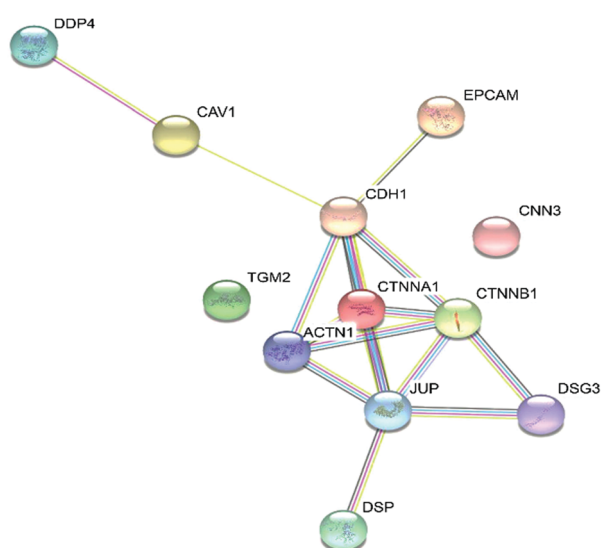


Fig. 4 The STRING network view of screened adhesion-related proteins. Colored lines between the proteins indicate the various types of interaction evidence.

We found that most of the screened proteins likely participate in direct or indirect interactions with each other. CDH1, CTNNB1, CTNNA1, and JUP are located at the core of the interaction network. Therefore, follow-up studies on adhesion function and establishment of MDCK suspension cells should include special attention to these proteins. Of particular interest is E-cadherin (CDH1), a classical epithelial adhesion protein that plays a key role in cell–cell adhesion.<sup>36,37</sup>

### Protein levels of E-cadherin and transglutaminase 2 were significantly reduced in MDCK suspension cells

E-Cadherin is an important cell–cell adhesion molecule and locate at the core position of the interaction network of selected proteins in this study. Transglutaminase 2 was the screening protein with the most significant difference in expression level between MDCK<sub>ADH</sub> and MDCK<sub>SUS</sub>. Therefore, western blot assay was used to further verify the protein levels of CDH1 and TGM2. As shown in Fig. 5, CDH1 and TGM2 protein levels in MDCK<sub>SUS</sub> cells were significantly lower than those in MDCK<sub>ADH</sub> cells. These results are consistent with iTRAQ and Realtime-PCR analysis results.

### Knockdown of CDH1 reduced the cell–cell adhesion of MDCK cells

We successfully obtained a CDH1 low-expression cell line (shRNA) by using lentivirus-mediated expression of CDH1 shRNA. Compared with untransfected MDCK cells (Blank) and vector control cells (shCon), both CDH1 mRNA and protein levels were significantly reduced in shCDH1 cells (Fig. 6A and B). Cell–cell adhesion assays demonstrated that shCDH1 cells had a significantly lower intercellular adhesion rate than shCon cells.

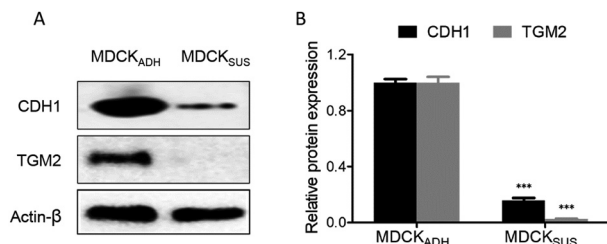


**Fig. 5** The relative protein expression of CDH1 and TGM2 revealed by western blotting. (A) Representative western blots of and CDH1 and TGM2, densitometrically quantified and normalised to  $\beta$ -actin. (B) Quantitation of western blots.

We observed no significant difference in adhesion between Blank cells and shCon cells (Fig. 6C). Fluorescence microscopy showed that the number of shCDH1 adherent cells was also significantly lower than that the shCon vector control cells (Fig. 6D). These results indicate that E-cadherin plays an important role in the intercellular adhesion of MDCK cells. This observation is consistent with the function of CDH1 in other cells.<sup>37</sup> In order to further verify whether shCDH1 cells affected viral replication, we analyzed the cell proliferation and influenza virus replication (Fig. 6E). The cellular growth curve revealed no significant difference in cell proliferation between shCDH1 and shCon cells. This finding suggests that inhibition of CDH1 does not affect the proliferation of MDCK cells. Our TCID<sub>50</sub> results show no significant difference in virus titer between shCDH1 cells and shCon cells, indicating that

inhibition of CDH1 does not affect the replication of influenza virus (Fig. 6F).

## Discussion

In this study, iTRAQ-based quantitative proteomics was used to analyze proteins with significant differences in expression between MDCK adhesion cells and suspension cells in order to identify MDCK cell proteins that function in cell adhesion. These proteins will become candidate targets for genetic engineering of MDCK suspension cells. Our results will support efforts to improve our understanding of cellular adhesion mechanisms. A total of 2973 proteins were quantified in the MDCK cell proteome. We identified 643 proteins with significantly different expression levels between MDCK<sub>ADH</sub> and MDCK<sub>SUS</sub> cells. Of these, 389 proteins were up-regulated and 254 proteins were down-regulated in suspension cells. Among the down-regulated proteins, 12 adhesion-related proteins were prioritized according to their functional annotation and predicted cellular localization. Protein expression changes were further verified by RT-qPCR to assess changes in mRNA expression of the selected genes.

Some of our prioritized proteins are speculated to play important roles in adhesion of MDCK cells. For example, E-cadherin (CDH1) is an adhesive transmembrane protein that consists of a large extracellular domain, a transmembrane domain, and an intracellular cytoplasmic domain and is a necessary component of adherens junctions in polarized epithelial cells.<sup>38,39</sup>

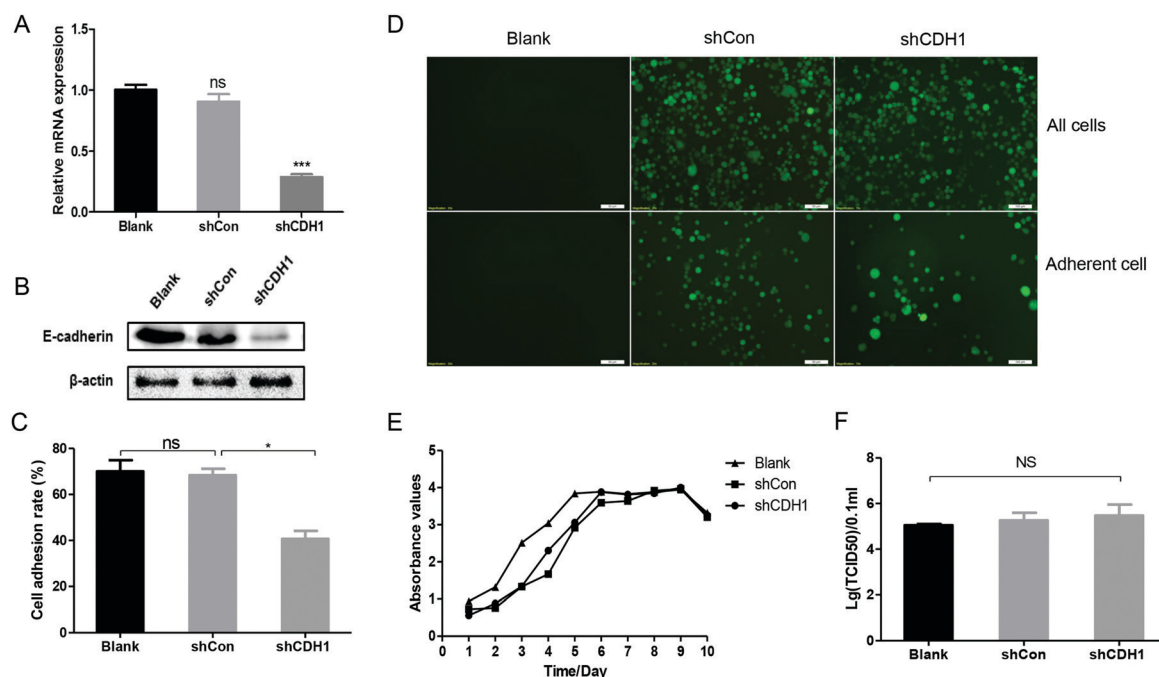


**Fig. 6** Verification of intercellular adhesion function of CDH1 in MDCK. (A) The relative mRNA expression of CDH1 by real-time quantitative PCR. Data are shown as mean  $\pm$  SD (standard deviation) of tissues from three separate individuals. Untransfected MDCK cells (Blank), vector control MDCK cells (shCon) and CDH1 RNAi MDCK cells (shRNA). (B) Representative western blots of CDH1, densitometrically quantified and normalised to  $\beta$ -actin. (C) Detection of the cell–cell adhesion rate by CCK8 method. (D) Detection of the cell–cell adhesion by fluorescence microscopy. (E) Effect of CDH1 low expression on cell growth viability. (F) Determination of titer of influenza virus H1N1 by TCID<sub>50</sub>.

E-Cadherin also plays important roles in cell migration and tumor suppression.<sup>15</sup> The cytoplasmic domain of E-cadherin binds to  $\beta$ -catenin and p120-catenin, and  $\alpha$ -catenin further combines with  $\beta$ -catenin at their N-terminal domains. The E-cadherin/catenin complexes stabilize adhesion junctions and support cell–cell adhesion. The extracellular domains of E-cadherin can bind to the extracellular domains of E-cadherin on adjacent cells and mediate adhesion connections between cells. The intracellular domains of E-cadherin bind to catenin proteins, which are responsible for connecting with the cytoskeleton and transducing intracellular signals.<sup>14,18,33</sup> Our experiments show that the expression levels of E-cadherin,  $\beta$ -catenin, and  $\alpha$ -catenin are all significantly reduced in MDCK suspension cells, suggesting that E-cadherin/catenin complexes also play an important role in MDCK cells. The cell adhesion result shows that CDH1 plays an important role in the intercellular adhesion of MDCK. Inhibition of CDH1 does not significantly affect the proliferative activity of MDCK and also does not inhibit the replication of influenza A virus H1N1. Thus, we believe that CDH1 can be used as a target gene for genetic engineering of MDCK suspension cells. As cell adhesion requires multiple adhesion molecules, it may be necessary to knock out several key proteins to obtain satisfactory suspension cells.

Cell–cell adhesion is executed mainly by three types of junctional complexes: tight junctions (TJs), adherens junctions (AJs), and desmosomes. Desmosomes are widely distributed along the lateral membranes of epithelial cells. They provide strong adhesion connections for epithelial cells and help to maintain stable tissue morphology.<sup>40</sup> Desmosomes are comprised of multiple proteins. In this study, we found that junction plakoglobin (JUP), desmoplakin (DSP), and desmoglein-3 (DSG3), which are all components of the desmosome complex, were significantly down-regulated in MDCK<sub>SUS</sub> cells. Desmoglein 3 (DSG3) is a type of desmosomal cadherin. Desmosomal cadherins are subdivided into DSG1–4 and DSC1–3. DSG3 is found mainly in epithelial cells. DSGs and DSCs are similar to classical cadherin; both contain highly conserved extracellular domains, a transmembrane domain, and an intracellular domain. They mediate intercellular adhesion by binding to other extracellular cadherins.<sup>41</sup> The intercellular domains of DSGs and DSCs interact with distinct sites in the central arm repeat domain of junction plakoglobin (JUP). JUP also interacts with the N-terminal plakin domain of desmoplakin (DSP).<sup>42</sup> The C-terminal domain of DSP interacts with the intermediate filaments of the cytoskeleton.

Multiple desmosomal proteins interact with each other to form a molecular chain that connects extracellular adhesion with the cytoskeleton and stabilizes intercellular adhesion. In this study, the desmosome components JUP, DSP, and DSG3 were significantly down-regulated in MDCK suspension cells, indicating that desmosomes on the surface of MDCK<sub>SUS</sub> cells were significantly reduced, and the adhesion between cells was weakened. Desmosomes are likely an important factor affecting cell adhesion in MDCK cells, and they should be considered candidate targets for obtaining MDCK suspension cells through genetic engineering.

In this study, transglutaminase 2 (TGM2) displayed the most significant down-regulation in suspension cells at both the

protein and mRNA level. TGM2 is a member of the transglutaminase family of ubiquitous multi-functional proteins. It displays cross-linking activity and also acts as a G-protein in signaling, and thus plays a vital role in wound healing, development, and cancer.<sup>42,43</sup> Studies have shown that TGM2 can positively regulate cell adhesion through multiple mechanisms. First, TGM2 can interact with extracellular matrix proteins and cell surface integrins to mediate cell adhesion to the extracellular matrix.<sup>43–45</sup> TGM2 is also involved in the formation of focal adhesions through influencing phosphorylation of paxillin and other focal adhesion proteins. Paxillin phosphorylation is important for recruitment and activation of other focal adhesion proteins.<sup>45,46</sup> However, the mechanism of regulation of cell adhesion by TGM2 is not yet fully understood. We found that TGM2 was significantly reduced in MDCK<sub>SUS</sub> cells, which likely contributes significantly to loss of adhesion in these cells. In addition, the expression of alpha-actinin-1 (ACTN1) was also significantly decreased in MDCK<sub>SUS</sub> cells. It has been shown that alpha-actinin-1 (ACTN1) can positively regulate organization of cell-matrix adhesion in keratinocytes.<sup>47</sup> The remainder of our prioritized proteins (CNN3, CAV1, DPP4, and EPCAM) are also known to function in cell adhesion, but their specific contributions to adhesion in MDCK cells are unknown.<sup>48–51</sup>

In this study, we report 12 newly identified cell adhesion-related proteins whose expression is significantly down-regulated in MDCK suspension cells. Among these adhesion-related proteins, inhibition of E-cadherin significantly reduced intercellular adhesion of MDCK cells. Moreover, the inhibition of CDH1 did not significantly affect the proliferation of MDCK cells and the replication of influenza virus. Thus, CDH1 can be used as a candidate target gene for modification of MDCK cell suspension. These findings provide a foundation for further research regarding the mechanism of epithelial cell adhesion and for the establishment of MDCK suspension cells by genetic engineering. Future studies should explore effects of these proteins on cell adhesion in MDCK cells and uncover how these proteins regulate cell adhesion.

## Conclusions

In this study, we report 12 newly identified cell adhesion-related proteins whose expression is significantly down-regulated in MDCK suspension cells. CDH1 participates in the intercellular adhesion of MDCK cells. These findings provide a foundation for further research regarding the mechanism of epithelial cell adhesion and for the establishment of MDCK suspension cells by genetic engineering. Future studies should explore effects of these proteins on cell adhesion in MDCK cells and uncover how these proteins regulate cell adhesion.

## Funding

This work was supported by the Major National Special Funds for Science and Technology (2015ZX09102016), the Fundamental Research Funds for the Central Universities (31920190004, 31920200069), the Program for Changjiang Scholars and



Innovative Research Team in the University (IRT\_17R88), and the Characteristic discipline of bioengineering construction for the special guide project of the “world-class universities and world-class disciplines” of Northwest Minzu University (11080306).

## Conflicts of interest

The authors have no conflicts of interest to declare.

## References

- N. Bardiya and J. H. Bae, *Appl. Microbiol. Biotechnol.*, 2005, **67**, 299–305.
- M. G. Pau, C. Ophorst, M. H. Koldijk, G. Schouten, M. Mehtali and F. Uytdehaag, *Vaccine*, 2001, **19**, 16–21.
- H. Ozaki, E. A. Govorkova, C. H. Li, X. P. Xiong, R. G. Webster and R. J. Webby, *J. Virol.*, 2004, **78**, 1–7.
- R. Youil, Q. Su, T. J. Toner, C. Szymkowiak, W. S. Kwan and B. Rubin, *et al.*, *J. Virol. Methods*, 2004, **120**, 23–31.
- O. W. Merten, H. Kallel, J. C. Manuguerra, M. Tardy-Panit, R. Crainic and F. Delpeyroux, *et al.*, *Cytotechnology*, 1999, **30**, 191–201.
- M. Taub, L. Chuman, M. H. Saier and G. Sato, *Proc. Natl. Acad. Sci. U. S. A.*, 1979, **76**, 38–42.
- S. Frisch and H. Francis, *J. Cell Biol.*, 1994, **124**, 619–626.
- M. Mochizuki, *Vaccine*, 2006, **24**, 4–8.
- A. Abdoli, H. Soleimanjahi, A. Jamali, P. Mehrbod, S. Gholami and Z. Kianmehr, *et al.*, *Biotechnol. Lett.*, 2016, **38**, 1–8.
- S. Kluge, D. Benndorf, Y. Genzel, K. Scharfenberg, E. Rapp and U. Reichl, *Vaccine*, 2015, **33**, 69–80.
- R. Van Wielink, H. C. M. Kant-Eenbergen, M. M. Harmsen, D. E. Martens, R. H. Wijffels and J. M. Coco-Martin, *J. Virol. Methods*, 2011, **171**, 53–60.
- T. Lecuit and P. F. Lenne, *Nat. Rev. Mol. Cell Biol.*, 2007, **8**, 33–44.
- H. Wolfenson, I. Lavelin and B. Geiger, *Dev. Cell*, 2013, **24**, 47–58.
- C. Guillot and T. Lecuit, *Science*, 2013, **340**, 5–9.
- C. M. Niessen, D. Leckband and A. S. Yap, *Physiol. Rev.*, 2010, 691–731.
- M. Lowndes, S. Rakshit, O. Shafriz, N. Borghi, R. M. Harmon and K. J. Green, *et al.*, *J. Cell Sci.*, 2014, **127**, 39–50.
- C. M. Van Itallie, A. J. Tietgens, A. Aponte, K. Fredriksson, A. S. Fanning and M. Gucek, *et al.*, *J. Cell Sci.*, 2014, **127**, 85–95.
- C. S. Chen, J. Tan and J. Tien, *Annu. Rev. Biomed. Eng.*, 2004, **6**, 275–302.
- C. Chu, V. Lugovtsev, H. Golding, M. J. Betenbaugh and J. Shiloach, *Proc. Natl. Acad. Sci. U. S. A.*, 2009, **106**, 2–7.
- V. Lohr, Y. Genzel, I. Behrendt, K. Scharfenberg and U. Reichl, *Vaccine*, 2010, **28**(62), 56–64.
- J. Capra and S. Eskelinen, *Lab. Invest.*, 2017, **97**(14), 53–70.
- D. Huang, L. Zhao and W. Tan, *Shengwu Gongcheng Xuebao*, 2011, **27**, 45–52.
- D. Huang, W. J. Peng, Q. Ye, X. P. Liu, L. Zhao and L. Fan, *et al.*, *PLoS One*, 2015, **10**, 1–11.
- L. F. Waanders, K. Chwalek, M. Monetti, C. Kumar, E. Lammert and M. Mann, *Proc. Natl. Acad. Sci. U. S. A.*, 2009, **106**, 2–7.
- S. Jin, H. Fu, S. Sun, S. Jiang, Y. Xiong and Y. Gong, *et al.*, *Comput. Biochem. Phys. D*, 2018, **26**, 5–7.
- C. Su, B. Zhang and W. Liu, *et al.*, *Oncol. Rep.*, 2016, **36**(2), 1048–1054.
- L. Reed and H. Muench, *et al.*, A simple method of estimating fifty percent endpoints, *Am. J. Epidemiol.*, 1938, **27**, 493–497.
- J. Shi, L. Zhang and Y. Lei, *et al.*, *Food Chem.*, 2018, **251**, 25–32.
- R. D. Unwin, J. R. Griffiths and A. D. Whetton, *Nat. Protoc.*, 2010, **5**(9), 1574.
- R. E. Sexton, G. Mpilla, S. Kim and P. A. Philip, *Semin. Cancer Biol.*, 2019, 1.
- I. Prada and J. Meldolesi, *Int. J. Mol. Sci.*, 2016, **17**, 1296.
- F. H. Brembeck and M. Rosa, *Curr. Opin. Genet. Dev.*, 2006, **16**, 51–59.
- M. Takeichi, *Curr. Opin. Cell Biol.*, 2018, **54**, 24–29.
- A. Ben-ze and B. Geiger, *Curr. Opin. Cell Biol.*, 1998, **10**, 629–639.
- G. Hopkins, T. E. Kimura and D. R. Garrod, *J. Invest. Dermatol.*, 2009, **127**, E12.
- A. R. Horwitz, *Nat. Rev. Mol. Cell Biol.*, 2012, **13**, 805–811.
- F. Roy, *Nat. Rev. Cancer*, 2014, **14**, 121–134.
- C. T. Capaldo and I. G. Macara, *Mol. Biol. Cell*, 2007, **18**, 189–200.
- F. van Roy and G. Berx, *Cell. Mol. Life Sci.*, 2008, **65**, 3756–3788.
- B. V. Desai, R. M. Harmon and K. J. Green, *J. Cell Sci.*, 2009, **122**, 4401–4407.
- D. Garrod and M. Chidgey, *Biochim. Biophys. Acta, Mol. Cell Res.*, 2008, **1778**, 572–587.
- R. Jones, B. Nicholas, S. Mian, P. Davies and M. Griffin, *J. Cell Sci.*, 1997, **110**, 2461–2472.
- E. Png, A. Hou and L. Tong, *Sci. Rep.*, 2018, **8**, 1–9.
- B. Tóth, Z. Sarang, G. Vereb, A. Zhang and S. Tanaka, *Immunol. Lett.*, 2009, **126**, 22–28.
- P. Evelyn and T. Louis, *Cell Adhes. Migr.*, 2013, **7**, 412–417.
- C. E. Turner, *Nat. Cell Biol.*, 2000, **2**, 231–236.
- K. J. Hamill, S. Hiroyasu, Z. T. Colburn, R. V. Ventrella, S. B. Hopkinson and O. Skalli, *J. Invest. Dermatol.*, 2015, **135**, 1043–1052.
- M. Nethe, E. C. Anthony, M. Fernandez-borja, R. Dee, D. Geerts and P. J. Hensbergen, *J. Cell Sci.*, 2010, **123**, 1948–1958.
- B. Joshi, S. S. Strugnell, J. G. Goetz, L. D. Kojic, M. E. Cox and O. L. Griffith, *Cancer Res.*, 2008, 8210–8221.
- A. Eapen, A. Ramachandran and A. George, *Cell Adhes. Migr.*, 2012, 307–311.
- S. V. Litvinov and H. Bakker, *J. Cell Biol.*, 1994, **125**, 437–446.